Optoelectronic Developments For Remote-Handled Maintenance Tasks in ITER

M. Van Uffelen [a], P. Leroux [a,b], F. Berghmans [a,c]

[a] SCK·CEN, Boeretang 200, 2400 Mol, Belgium
[b] KHK Geel, Kleinhoefstraat 4, 2440 Geel, Belgium
[c] Vrije Universiteit Brussel, Pleinlaan 2, 1050 Brussels, Belgium

mvuffele@sckcen.be

Abstract

Remotely handled maintenance tools operated in the future International Thermonuclear Experimental Reactor (ITER) will face a harsh radiation environment, with total dose level requirements of several MGy. Optical fiber data communication has been considered as an alternative to conventional electronic transmission between the control room and remote handled maintenance equipment, mainly owing to its insentivity to electro-magnetic interference and to its wavelength encoded multiplexing capabilities. In this paper we summarise main results obtained at SCK•CEN over the past years towards the development of radiation tolerant fibre-optic communication links and report on the radiation tolerance of various individual optical components such as optical fibres, laser diodes and photodetectors, as well as their associated electronic driver circuits.

I. ITER Background

The main goal of ITER, i.e. 'the way' in Latin, is to demonstrate the feasibility of a fusion power plant to generate electrical power. It is a tokamak, in which strong magnetic fields confine a torus-shaped plasma of about 500 MW fusion power (cf. Figure 1).

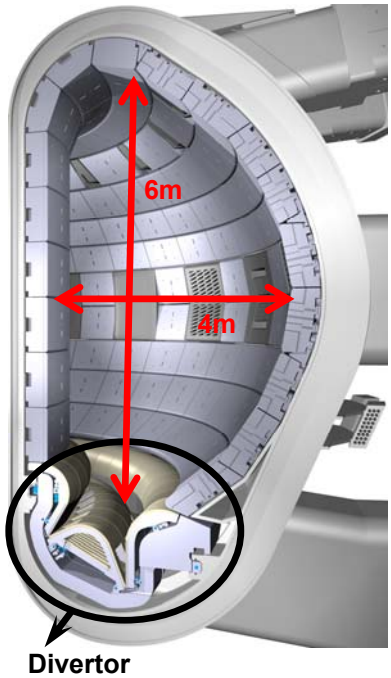

Figure 1 : Cross-section of a D-shaped torus in which a plasma will be generated and heated, hence creating conditions for fusion reactions to occur. The modular divertor elements sit at the bottom.

In-vessel first wall components in the future ITER reactor will be subject to plasma-wall interactions causing activation and erosion. This calls for regular refurbishment, depending on the erosion rate. Furthermore components may need to be replaced due to unexpected failure. Therefore common and dedicated remote handling (RH) equipment for repair and maintenance tasks are needed, which will have to withstand harsh radiation environments [1]. . Besides the very high total dose levels, ITER brings along large masses to be manipulated in a complex geometry of movement with stringent positioning accuracies. Such systems are not readily available from other fields such as underwater, space, or nuclear fission applications.

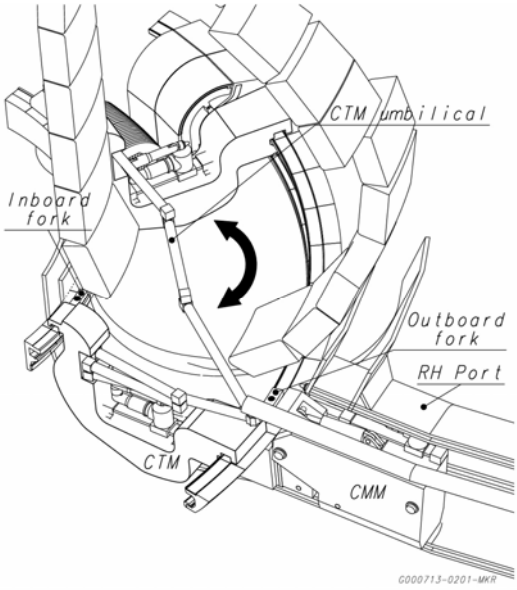

Figure 2 : The ITER in-vessel cassette handling scheme. (Note. CTM shown at both entry and deployed positions).

From the earliest research and design efforts among the different international ITER partners, the European home team has generously contributed to the development of the divertor system and its maintenance scenarios [3]. The most important function of the divertor system is to exhaust the major part of impurities and other particles from the plasma [4]. As the main interface component under normal operation between the plasma and material surfaces, it must tolerate high heat loads while at the same time providing neutron shielding for the vacuum vessel and magnet coils in the vicinity of the divertor. The replacement of the divertor and its refurbishment in a hot cell are foreseen a few times during the ITER lifetime. To meet this requirement, a cassette-type divertor has been selected, which will be replaced and transported with the help of different tools, such as the

Cassette Multifunctional Mover (CMM) and the Cassette Toroidal Mover (CTM), as illustrated in Figure **2**. Conservative estimations of the activation levels made during the final design show that the RH equipment will be exposed to ionizing dose levels of 1-10 MGy and temperatures up to 200 °C [5].

Connecting remotely operated actuators and sensors with the control room conventionally requires bulky and shielded umbilicals. Their size could be reduced by applying radiation tolerant communication links with multiplexing capabilities. Fibre-optic technology is considered as a potential EMI-free solution, since individual components such as optical fibres and couplers, light emitters and photo detectors have thus far shown promising results up to MGy dose levels [6],[7],[8]. The long-term reliability of optical fibres and cables also depends on the evolution of their mechanical properties, information about which only little is known from literature at MGy dose levels. Furthermore, the driving electronics necessary for controlling either the semiconductor light-emitting or light-receiving devices up to these high total dose levels is not commercially available. Over the past several years we therefore focussed our efforts on assessing the optical and mechanical radiation tolerance of optical fibres, on studying radiation effects on different state-of-the-art laser diodes, and on designing and developing dedicated electronic drivers. This paper is hence structured as follows. After dealing with a number of experimental details in the next section, we highlight our recent results on optical fibres, on opto-electronic transmitters, as well as our irradiation experiments with photodiodes, and finally summarize our latest results on driving electronics, from discrete components to ASICs.

II. Experimental details

All irradiations are performed in the facilities of the Belgian Nuclear Research Centre SCK·CEN. Different gamma irradiation facilities are operated using mainly sealed ^{60}Co sources. They offer a wide gamma dose rate ranging from 0.1 Gy/h up to 80 kGy/h, environmental control (e.g. heating up to 200 °C) and on-line instrumentation [9]. Neutron irradiations of remote-handling components are performed in the BR1 reactor, which is a gas-cooled and graphite moderated reactor, fuelled with natural Uranium [10].

The radiation assessment of single mode optical fibres was achieved with in-situ radiation-induced attenuation measurements in the range of 1.2 µm – 1.7 µm, with the help of a tuneable laser source and a photodetector. The mechanical properties were measured before and after irradiation with both tensile tests and strength measurements, at two different facilities for comparison, i.e. at the Draka Comteq facilities in Eindhoven (The Netherlands), and at the University of Birmingham (UK). The dynamic stress corrosion susceptibility of the samples was determined by the two-point bending method, according to the IEC 60793-1-33 standard (method B). This method is used to determine the strength (50% failure stress σ_f) and the dynamic fatigue factor (stress corrosion parameter, n_d), particularly for high strength optical fibres.

InGaAs photodiodes were also characterized in-situ, before, during and after irradiation. We measured the dark current, as well as their wavelength dependent photocurrent between 0.98 µm and 1.65 µm.

More recently, long-wavelength VCSELs, emitting in the 1.4 µm – 1.7 µm range were also evaluated. We recorded before and after irradiation the output optical power and the forward voltage as a function of both the injected current and temperature between 20 °C and 50 °C, using a laser diode controller from ILX Lightwave (model ILX LPA-9080) and an optical integrating sphere for measurements (model ILX OMH-6745B). During irradiation, the devices were unbiased, which left them in worst case test conditions, since current annealing is not allowed.

Finally, various Si-based transistors, including Si and SiGe bipolar transistors, as well as CMOS transistors were assessed up to MGy dose levels with in-situ measurements of their output characteristics and other main parameters.

The main results obtained with this list of passive and active photonic components and their associated driving electronics is presented in the following 3 chapters.

III. Passive fibre optical components

The main long-term effects induced by ionizing radiation on passive fibre optical components are wavelength dependent optical losses and a mechanical degradation of their protective packaging (polymer coating) materials.

A. Radiation induced attenuation in optical fibres

The typical radiation induced attenuation (RIA) in optical fibres measured in-situ in different commercially available multimode fibres is illustrated in Figure 3. It is well known that the RIA, commonly expressed in dB/km, depends on many environmental parameters such as total dose, dose rate and temperature, …, but also on various fabrication parameters including the glass composition and coating materials as well as the fibre drawing speed and tension.

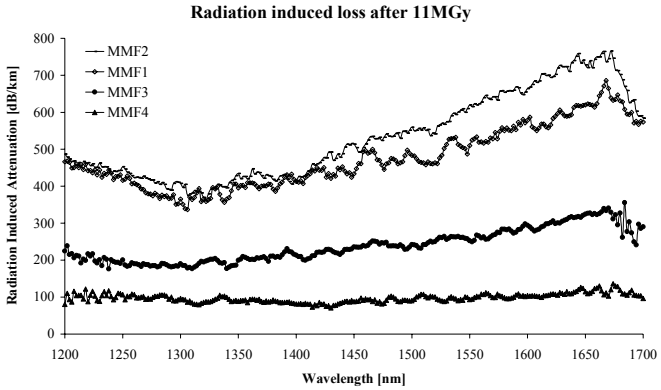

Figure 3 : radiation induced optical losses as a function of wavelength, measured in-situ in 4 different commercially available multimode fibres after a cumulated dose of 10.7 MGy

While these gradient index fibres were exposed at a dose rate of 15 kGy/h up to a cumulated dose of 10.7 MGy at a controlled temperature of 60 °C, their RIA can vary between 0.1 dB/m and 0.8 dB/m. We also observe that at these total

dose levels, the operating wavelength is best chosen in the 1.3 µm region, except for the least sensitive fibre MMF 4, which presents a RIA that is almost wavelength independent.

B. Mechanical degradation of optical fibres

In addition to the numerous assessments presented in literature of the radiation-induced optical property changes in optical fibres, we investigated the impact of MGy dose levels on the mechanical properties of different single and multimode fibres . We compared the tensile test and two-point bending test results with commercially available optical fibres before and after irradiation up to 15 MGy [14].

Figure 4 presents tensile tests results obtained with a standard single mode fibre exposed to different total dose levels and which are compared with an identical sample that was only thermally aged. The 95 % confidence limit (vertical bars) was calculated using a t-distribution. It is clearly seen, in comparison with the thermally aged samples, that the average strength drops with increasing radiation dose beyond 1 MGy. Our results show a significant strength reduction of about 50 % at higher dose levels, relevant for particular applications in nuclear power facilities and in future large nuclear physics experiments. The width of the distribution in the confidence limit also increases. Moreover, the Weibull distribution (not shown here) indicates that the increase of the dose causes the creation of a second failure mode, which is responsible for the decrease in strength and the increase in the standard deviation. This radiation effect can be related to the nucleation of flaws on the surface of the fibre if the fibre is flawless and/or the growth of the flaws size. It can also explain the radiation-induced presence of the second failure mode in the Weibull distribution.

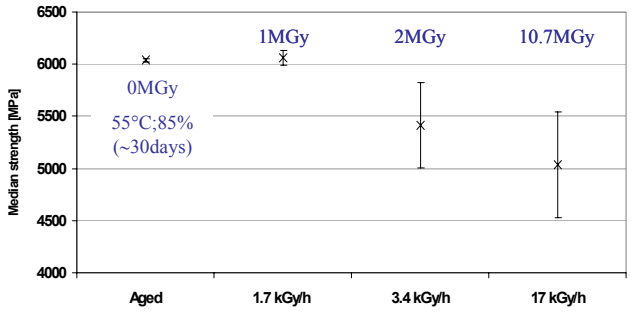

Figure 4: The average strength of four differently treated samples of a single mode fibre. Also shown is the 95 % confidence limit calculated using the t-distribution. (Measurements performed at Univ. of Birmingham.) [14].

In order to better understand the cause of degradation under radiation, the fibre was stripped from its coating using hot sulphuric acid. The mechanical strength reduction observed seems to depend on both the coating materials and the test conditions, as suggested by the roughening of the outer glass surface of the optical fibre, observed with atomic force microscope (AFM) images and illustrated in Figure **5**. The mean square roughness (a) before irradiation was 0.537 nm and (b) increased drastically to 3.314 nm after the combined thermal-radiation treatment. The surface roughness can act as cracks or flaws at the surface and hence explain the observed weakening.

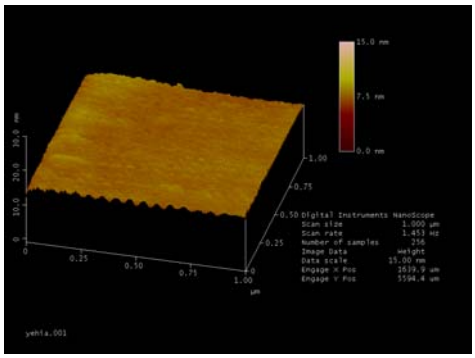

(a)

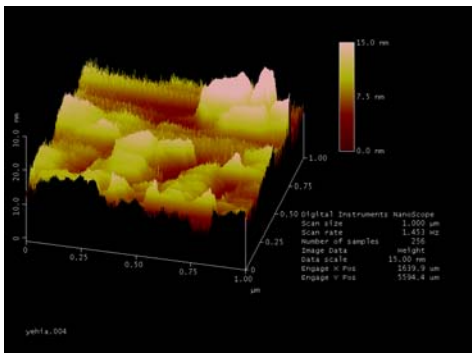

(b)

Figure 5 : AFM pictures of the glass surface of a single mode fibre (a) before and (b) after irradiation up to 15 MGy. The increase in surface roughness is the cause in the lower strength of the fibre.

IV. Active Photonic Components

A. P-i-n type Photodetectors

COTS photodiode assemblies were evaluated under radiation for their use in bidirectional fibre optic links [8]. Si and InGaAs PDs were assessed up to 10 MGy, and the Si PDs were also exposed to a thermal neutron fluence of about 10^{15}n/cm^2, as illustrated in Figure 6.

Figure 7 presents the radiation-induced increase of the dark current measured at a reverse bias of -5 V for InGaAs photodiodes. During irradiation we observe a substantial monotonous increase of the dark currents, as compared to the more limited growth observed for the Si photodiodes. At a cumulated dose of 10 MGy, the dark currents have grown by a factor 500 to 700, while the growth does not show any sign of saturation as opposed to the Si-PD's. When the irradiation is halted, the dark currents decrease promptly by about 10-20% (1-1,5 µA at -5 V), which can be interpreted as a radiation-induced current in the PD [8]. After almost 4 days of recovery at 60 °C, the dark currents are monitored at different temperatures between 40 °C and 70 °C. When the temperature is again raised to 60 °C, we observe a limited reduction of the radiation induced dark currents by about 5-10%. These iso-thermal measurements can be used to verify the long term reliability (wear-out) of the photodiodes under radiation. The authors in [17] demonstrate that for gamma doses of 100 kGy, this radiation damage does not affect the wear-out rate of the devices and hence that it has no impact on their long term reliability.

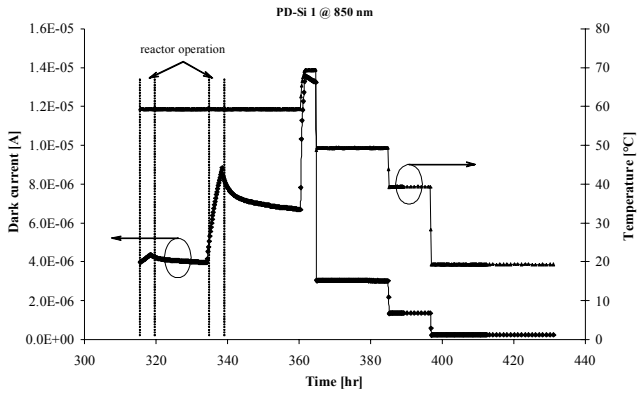

(a)

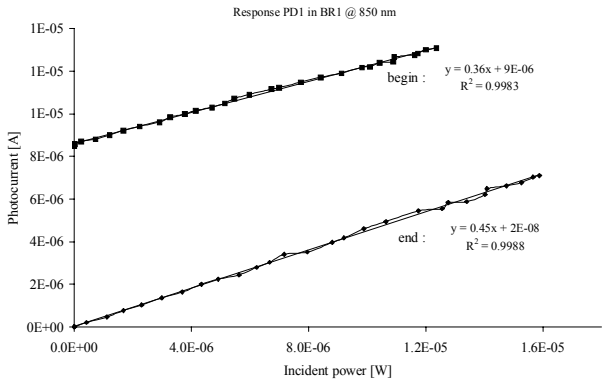

(b)

Figure 6 : (a) Evolution in time of the dark current in a Si PD at the end of the experiment in the BR1 reactor and during the subsequent isothermal recovery test. (b) Response of a Si-PD before and after the exposure to a thermal neutron fluence of $7 \cdot 10^{15} n/cm^2$ and a background gamma dose of 20 kGy. Note : these PD's were first gamma irradiated up to a cumulated dose of 2 MGy.

We also monitored in-situ the wavelength dependence of the photodiode response, in order to verify whether wavelength multiplexing possibilities were still within reach. We observe no catastrophic failure for any of the InGaAs devices nor for the Si devices at these total doses, and their response remains linear. Our in-situ measurements also show that ionizing radiation damage has no significant influence on the wavelength dependence of the photodiode response in the region of interest, which should allow the use of coarse wavelength division multiplexing (CWDM) architectures under high gamma doses.

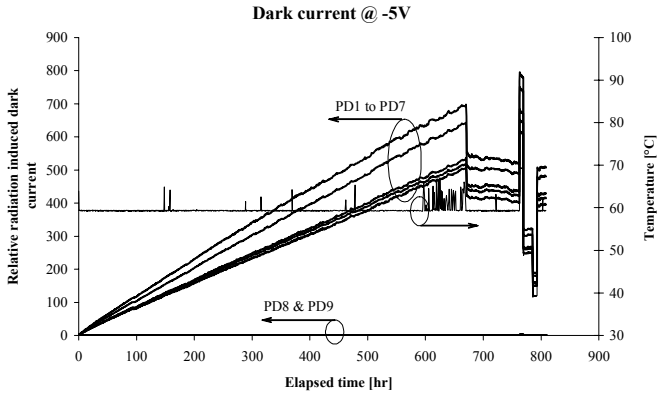

Figure 7: Relative increase of the dark currents measured as a function of time for 7 InGaAs-PD's at a reverse bias of -5 V, a gamma dose rate ~ 15 kGy/h, temperature 60 °C. PD 8 and PD 9 were used as reference, outside the irradiation container.

In conclusion, both dark current increase and responsivity decrease characterize the photodiodes main degradation mechanism, with the former effect dominating. Moreover, the damage resulting from displacement effects caused by neutrons is much more significant in comparison with the damage observed under gamma radiation as observed by many other authors (e.g. [18],[19]). In the absence of neutrons, which are only considered for ITER maintenance tasks if the maintenance equipment has to be stored inside the bio-shield during plasma burns, one should prefer the use of Si photodiodes rather than InGaAs devices to build communication links that can withstand total doses up to 10 MGy, since their dark current increase is much more limited.

B. Surface-emitting Laser diodes

1) Multimode VCSELs

We first reported on high total dose gamma and neutron irradiations of 850 nm vertical-cavity surface-emitting laser (VCSEL) assemblies at a constant temperature of 60 °C [20]. The devices confirm their excellent tolerance to gamma radiation up to a total dose of 20 MGy, obtained in 2 steps of 10 MGy. The optical power loss at nominal forward current is below 2 dB, the threshold current remains unaltered and no influence on the I-V characteristics can be seen. Applying a continuous forward bias to the VCSELs seems beneficial in terms of a lower optical power loss. There is no sign of recovery in the 24 hours following both 10 MGy irradiation stages. The results stress the importance of conducting in-situ experiments, of controlling the bias of the VCSELs in between measurement cycles and they also emphasize the need to take specific care for the design of the VCSEL assembly.

A neutron irradiation was then conducted up to a total fluence on the order of 10^{15} $n \cdot cm^{-2}$, at a constant ambient temperature of 60 °C. The devices here were new unlensed VCSEL assemblies as well as those previously exposed to the 20 MGy gamma dose. As illustrated in Figure 8, the devices experience a dramatic increase of the threshold current which rapidly exceeds the nominal operating forward current. This results in an almost 100 % optical power loss at I_f = 15 mA for fluence levels of a few 10^{15} $n \cdot cm^{-2}$. VCSELs previously exposed to gamma rays exhibit an accelerated degradation under neutron radiation compared to not pre-irradiated devices (not shown here). This conclusion should be taken with specific care as the pre-irradiated VCSELs were obtained from another manufacturer, but it indicates that care should be taken when interpreting results for mixed ionizing-particle radiation environments. The beneficial effect of applying a continuous forward bias to the VCSELs during the irradiation is also evidenced. In contrast to the gamma radiation, the (I,V)-curves are now also affected by the neutrons. Again, the behavior of the (I-V) characteristics is different for the pre-irradiated and the unirradiated devices.

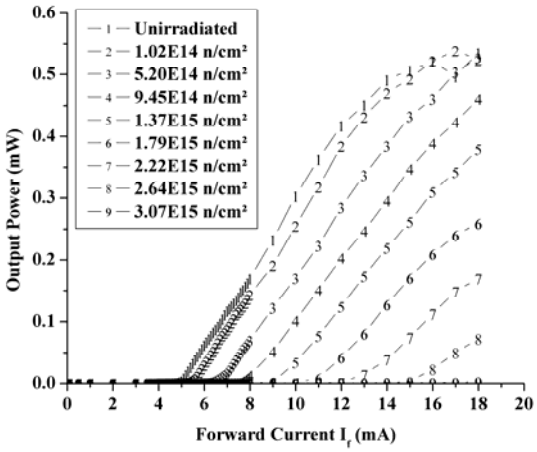

Figure 8: P-I curves of a 850 nm VCSEL assembly at different neutron fluence levels and 60.0 °C ± 1.5 °C.

Since the VCSEL assemblies still operate in a satisfactory way at this 20 MGy gamma dose and at a 10^{14} n•cm^{-2} neutron fluence level, we believe that they are excellent optical emitter candidates for fiber-optic communication links in ITER.

2) Long-wavelength VCSELs

As an alternative to multimode links, one also needs to assess the radiation behaviour of state-of-the-art single mode VCSELs that became recently available, since they would allow a more straightforward optical MUX architecture with largely deployed fibre optic components.

We preformed a first gamma radiation assessment of long-wavelength VCSELs emitting in the 1,4-1,7 µm region, up to 10.1 MGy [22]. The results obtained for a 1.52 µm VCSEL are shown in Figure 9. We observe only a very limited damage, which is somewhat more pronounced at lower temperatures, which suggests a thermally activated recovery. The ionizing radiation induces an increase of the threshold current and a reduced output efficiency. Their temperature dependence is shown in Figure 9 (b). The difference in temperature dependence of both the current gain in the active region and the cavity resonance explains the intrinsic non-linear relation of the threshold current and the output efficiency with temperature. At 25 °C, the threshold increases by 9 %, while the efficiency drops about 6 %. This radiation damage is generally attributed to non-radiative recombination centres, which are created in the active region through displacement damage, requiring an increased forward current before the device starts to lase, but with no significant effect on the slope efficiency. However, the temperature dependence in Figure 9 (b) suggests that there are two competing radiation-induced mechanism, since the threshold changes become less significant at higher temperatures, contrary to the slope efficiency which further decreases as the temperature is raised to 50 °C. This was confirmed by analysing the (I,V)-curves in more detail in [22].

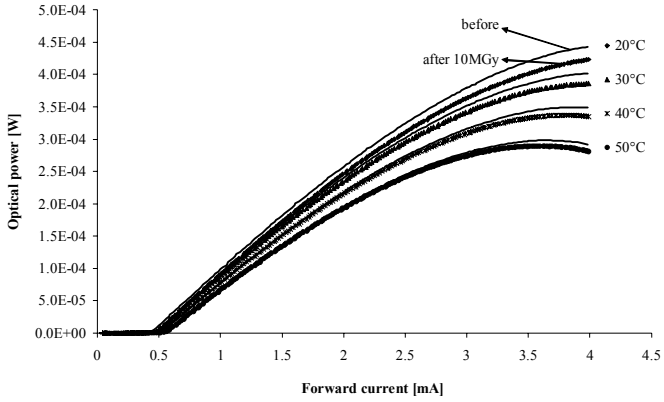

(a)

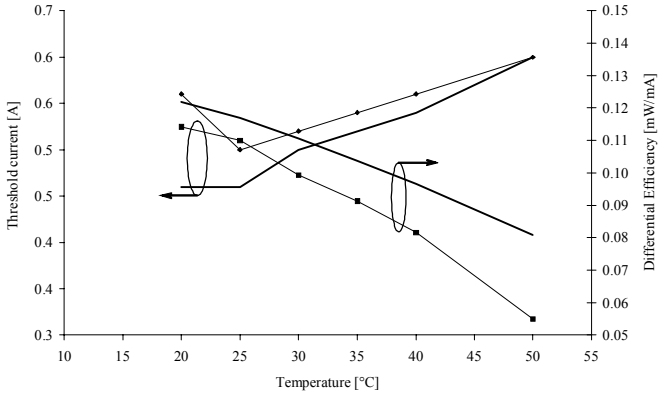

(b)

Figure 9: (a) The (L,I)-curves measured between 20°C and 50°C before (solid lines) and after irradiation up to 10 MGy (dotted lines) for a TO-46 canned VCSEL operating at 1,52 µm. and (b) the threshold increase (left axis) and decrease of output efficiency (right axis) as a function of temperature before (solid lines) and after irradiation (dotted lines).

V. RADIATION TOLERANT DRIVING ELECTRONICS

Robust fibre optic transmission systems up to MGy dose levels require the development of associated electronic circuits, such as laser drivers and amplifiers for the photodiodes. Our first designs were assembled and assessed using discrete bipolar transistors. Later on, this allowed us to migrate towards ASICS.

A. Discrete commercially available transistors

1) Si bipolar transistors

We first developed a VCSEL driver based on discrete Si bipolar transistors (cf. [15] and references therein). The design was based on an adapted SPICE model of the COTS transistor, that described the radiation induced damage as a supplementary time-dependent base current and hence a reduced current gain, and a time-dependent diminishing collector-emitter saturation voltage. This driver consisted of a consists of a current source and a differential amplifier. The driver uses standard TTL input signals and delivers a forward current of 12 mA to a pigtailed 840 nm VCSEL. SPICE simulations show that the driver still delivers a sufficient forward current to the VCSEL, in spite of the radiation induced degradation of the hfe and VCEsat values of the

transistors. These simulations were verified by our experiments. At a total dose of 1 MGy, the measured decrease of the forward current was only about 8 %. During this experiment, we transmitted digitized and serialized data from position sensors with both this optical transmitter and with an LVDS (Low-Voltage Differential Signaling) transmitter. It allowed us to compare the performance of both transmission schemes up to 4.5 MGy [23].

In an attempt to build a robust bi-directional multimode link with these VCSELs, we also assessed a fibre optic transmitter, consisting of a pulse-width modulator (PWM), a rad-hard current driver (cf. also further) and a VCSEL [16]. These assemblies were irradiated up to 10 MGy at 60 °C. As illustrated in Figure 10, our in-situ measurements with carrier signals at 5 kHz and 30 kHz show that this link is a suitable option for the transmission of slowly varying sensor signals (e.g. temperature, position, ...) in a harsh environment, with optical multiplexing possibilities.

The degradation of the driver current source is illustrated in Figure 10 (a). These data were acquired with a trigger signal of 5 kHz and an input voltage of 4.2 V. We observe a small increase of the duty cycle, which can be attributed to the behaviour of the PWM. Furthermore, the high and low output current levels have each evolved by a few percent [16]. The higher level has dropped monotonously by about 8 % after 10 MGy, whereas the lower level has grown with 4 %. The former is attributed to a degradation of the current source, whereas the latter could be explained with a leakage current increase in the output stage of the driver. Nevertheless, this driver circuit hardened by design still functions properly and is yet able to forward a current that will turn the optical emitter on or off. The post-irradiation measurements show also a limited recovery of about 2 % in 3 days.

The degradation of the VCSEL output is presented in Figure 10 (b). We observe a total loss of 60-80 % (4-7 dB) for 3 DUTs, which shows a dispersion common to COTS devices, and confirms our earlier results [21]. The overall radiation induced loss stems from the individual contributions measured separately and during previous experiments, which can be attributed in part to the driver current source and its amplifying stage, as well as to the optical power losses in the pigtailed laser diode. Hence, we do not observe additional radiation damage due to the system integration.

2) SiGe heterojunction bipolare transistors (HBT)

Unfortunately these Si BJT's are currently no longer available. A viable alternative was sought in a VCSEL driver based on bandgap-engineered SiGe Heterojunction Bipolar Transistors (HBT's) [24], for which we first adapted a SPICE model to include radiation damage [25], and which was recently extended with a more physically based description [26]. The model is based on the presumably dominant physical degradation mechanism, obtained from early experiments which showed that the reduction in current gain owes to an increase in Shockley-Read-Hall recombination in the base-emitter space charge region. This is due to the production of G/R-centers caused by radiation induced lattice defects. As a consequence, the base current of the transistor is increased. This presumption is supported by the fact that the excess base current during irradiation has been shown to be inversely proportional to the square root of the collector current. This insight was used to reduce the model complexity to only five coefficients. The resulting model has a very broad range of validity covering the entire design-space of interest.

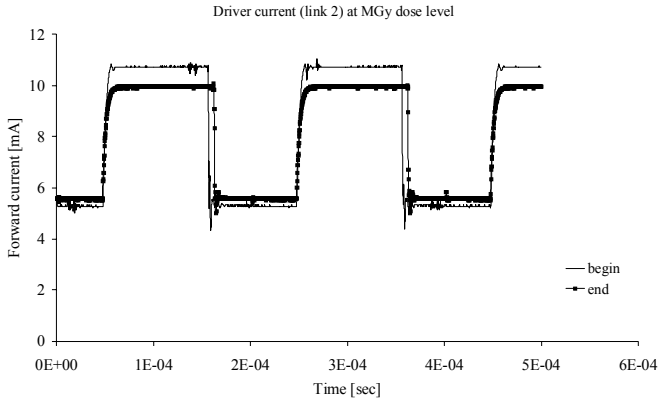

(a)

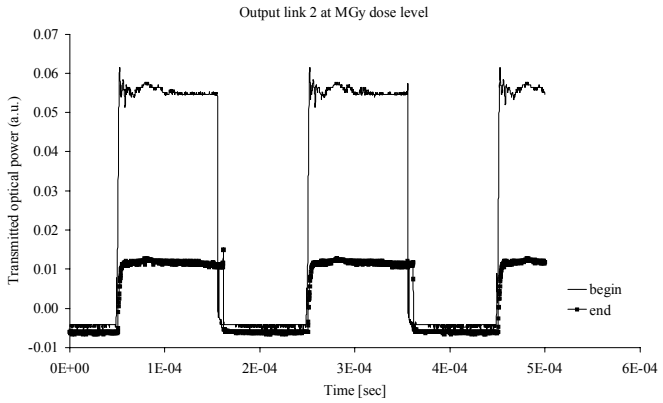

(b)

Figure 10: (a) Comparison of the pre- and post-irradiation output signals of the current driver circuit, at 60°C. (b) Comparison of the pre- and post-irradiation output signals of the optical emitter (VCSEL).

A digital VCSEL driver was then realized using these discrete SiGe HBT's (cf. Figure 11). Simulations, based on the SPICE model developed in [26], were used to design the circuit and predict its behavior under radiation. Note that by adding a diode (D_1) in the divider chain largely reduces this temperature dependence. Simulations predicted a current increase of only 2 % when temperature is raised from 20 °C to 90 °C; a reduction by a factor 10 compared to pure resistive biasing.

The driver tolerates high levels of gamma radiation, up to a total dose of 12 MGy, and features less than 2 % drift in the forward current of the VCSEL. The output duty cycle measured in-situ showed about 1 % decrease at 200 kHz.

Off-line measurements were performed to describe and explain the circuit's operation at elevated temperatures. Before irradiation, the output current of the driver (12 mA at 25 °C) increases less than 1 % up to a temperature of 85 °C which fits well with our simulations. After irradiation, the temperature tests revealed a recovery effect which is linked to the recovery of the individual transistors' current gain. Finally, measurements at an operation frequency of 10 MHz have demonstrated the usefulness of the SiGe transistor and particularly of this design for low frequency optical

communication in extremely harsh radiation environments, up to 10 MGy.

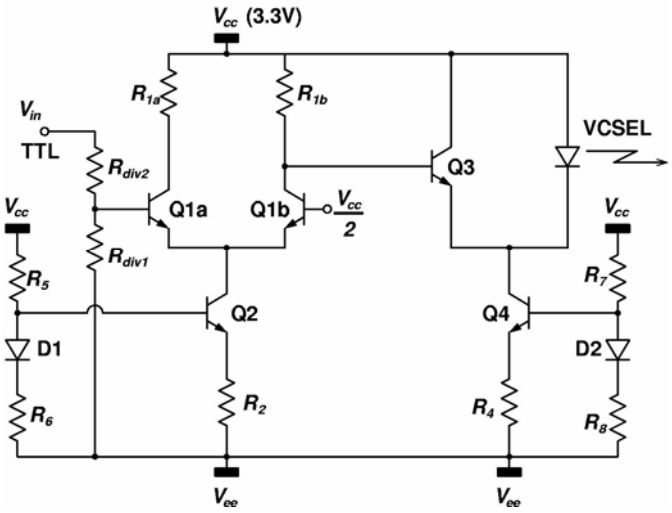

Figure 11: Schematic diagram of the proposed SiGe HBT-based circuit-hardened digital VCSEL driver.

B. Towards radiation tolerant IC's

As a first step towards further miniaturization, we designed a TTL compatible CMOS VCSEL driver as a fully integrated alternative to the discrete SiGe VCSEL driver presented in the previous section. The circuit can operate at least up to a frequency of 155 Mbps and is hence suited for the SONET OC-3 standard. This circuit was implemented in a mainstream 0.7 µm CMOS technology. The design of the circuit tackles the damaging radiation effects both at circuit and layout level. For the layout a dedicated component library was built. The circuit features a replica based current correcting feedback mechanism (cf. Figure 12) for compensation of radiation induced shifts in the device characteristics [27].

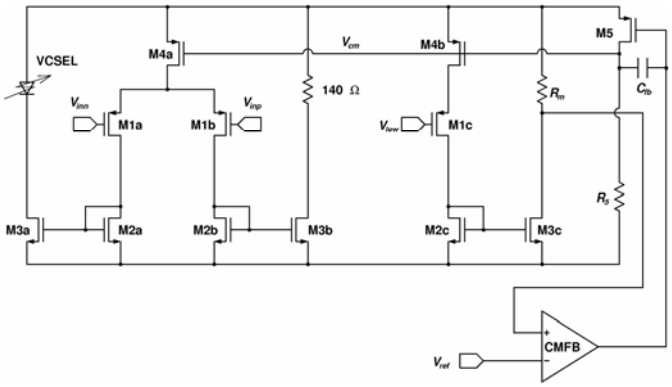

Figure 12: Schematic of the TTL compatible CMOS VCSEL driver.

Note that the input differential pair was implemented with PMOS transistors as is current source transistor M4a. The latter holds the main reason for this choice. The threshold voltage of this PMOS transistor can only decrease in response to radiation. This observation allows optimization of the feedback mechanism which aims to keep the value of this current constant.

Low dose rate experiments with DIL40 packaged driver IC's up to a total dose of 3.7 kGy (370 krad) have shown that the 90 % decrease in VCSEL current without the feedback loop is limited to only 2 % when the feedback is included. The eye diagram of the circuit at 155 Mbps showed no apparent degradation. A complementary experiment at a dose rate of 21 kGy/hr up to a total dose of 13.5 MGy has shown that the VCSEL current only drops by 10 % after a TID of 3.5 MGy (350 Mrad). This is illustrated in Figure 13, which compares the relative VCSEL current from the driver output in the on-state as measured in-situ, during irradiation, with and without the feedback.

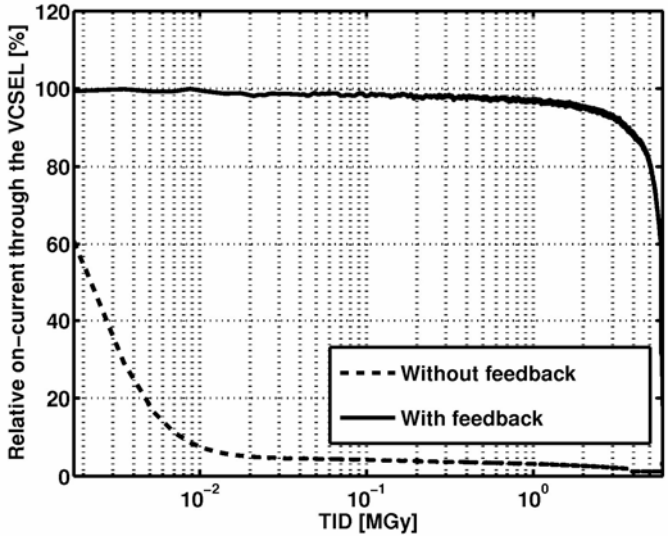

Figure 13: Measured relative VCSEL current from the driver output with the feedback network either activated or disabled. Dose rate of 21 kGy/hr.

Again, the circuit loses functionality quickly when the correcting feedback circuit is disabled. The output current through the VCSEL has already dropped to 60 % when the first measurement is taken after the irradiation started. It drops further to 10 % after 8 kGy. With the feedback network enabled, the output current drops only 10 % after 3.5 MGy. The circuit starts to break down and looses its functionality completely after 6 MGy.

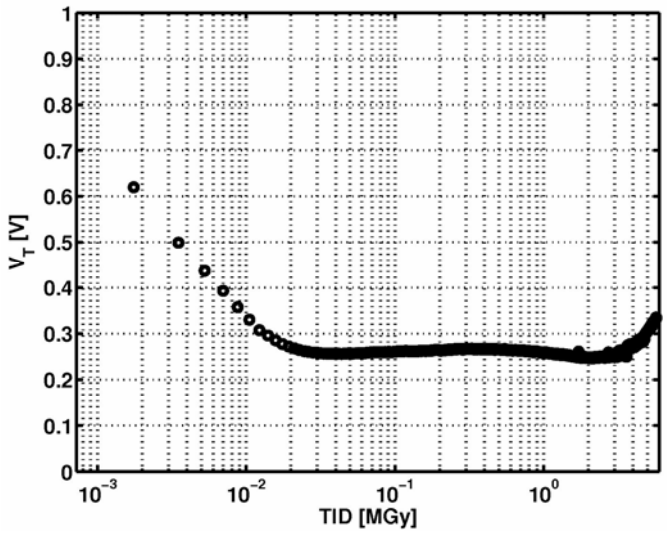

Figure 14: NMOS threshold voltage V_T as a function of TID. Dose rate of 21 kGy/hr.

The threshold voltage is plotted as a function of accumulated dose in Figure 14. For cumulated doses below 100 kGy, we obtain a reduced V_T. This is caused by the rising number of positively charged hole traps in the gate oxide which 'helps' to turn on the transistor. After roughly 3 MGy,

the V_T starts to increase again. This rebound is known to be caused by an increase in the number of negatively charged interface states at the boundary between the Si channel and the SiO_2 gate oxide. These negative charges counteract the positive holes, trapped in the gate oxide and hence cause an increase in V_T. Our results also suggest a decreased mobility for the electrons in the channel, tentatively explained as a result of lattice defects created by high-energy compton electrons.

Depending on the envisaged application, more advanced integrated technologies could be considered as well, such as strained Si and SOI, which have even smaller feature sizes (65 nm and below). The applied tensile-strain inducing techniques boost the device performances as they increase the mobility of electrons, which is particularly of interest to NMOSFETs. Initial proton irradiations were performed, where a global technique using strained SOI was compared to a local technique, where strain is induced by a strained Contact Etch Stop-Layer (sCESL) [28]. These results have shown that irradiation has a different impact on some device characteristics, such as the threshold voltage shift and the behaviour of the parasitic back-channel transistor, depending on which tensile-strain-inducing technique is used. The main effect of proton irradiation is the creation of interface traps and positively charged holes trapped in the buried oxide. It was shown that the combination of strained Si with sCESL on a NMOS device will lead to the lowest radiation sensitivity, whereas PMOSFETs have a better radiation behavior when a strained Si-channel is used. For practical PMOS transistors, it is only relevant to evaluate the tensile strained Si, because in practice a compressive sCESL will be used instead of the tensile sCESL, which was studied in this paper. While these results are relevant for potential space applications, the high dose radiation assessment of these strained technologies is still to looked at.

VI. Summary

Maintenance tasks in the future ITER reactor will have to be performed in harsh radiation environments, requiring robust instrumentation and control equipment that can withstand MGy dose levels. Opto-electronic communication links between these maintenance tools and the control room present an interesting option as they would offer wavelength-encoded multiplexing possibilities. In this paper we summarized the main results obtained at SCK•CEN over the past years towards the development of radiation tolerant fibre-optic communication links, including the individual optical components such as optical fibres, laser diodes and photodetectors, as well as their associated electronic driver circuits. As our current efforts aim at further miniaturization and integration with rad-hard ASICs, the ITER community should benefit from their potential use in other radiation environments, such as the future SLHC, which will impose higher radiation levels to the equipment used up to several MGy. This possible common market supports the interest of a shared R&D program for future developments of O/E communication links for both high energy physics experiments and thermonuclear fusion reactor applications.

VII. Acknowledgements

The authors are grateful to all contributing partners, and particularly Gerard Kuyt, Piet Matthijsse and Elise Regnier from Draka, Yehia El Shazly and Stephen Kukureka from the University of Birmingham, Cor Clays and Eddy Simoen from IMEC, Pentti Karioja, Antti Tanskanen and Veli Heikkinen from VTT and Sofie Put from SCK·CEN.

This work, supported in part by the European Communities under the contract of Association between EURATOM/Belgian State, was carried out within the framework of the European Fusion Development Agreement. Part of the work is also supported by the EU FP6 Network of Excellence on Micro-Optics NEMO. The views and opinions expressed herein do not necessarily reflect those of the European Commission.

VIII. References

[1] http://www.iter.org
[2] ITER Plant Description Document, Chapter 2.9 "Remote Handling Equipment ", ref. G A0 FDR 1 01-07-13 R1.0, July 2001.
[3] J.Palmer, M.Siuko, P.Agostini, R.Gottfried, M.Irving, E.Martin, A.Tesini, M.Van Uffelen, "Recent developments towards ITER 2001 Divertor Maintenance", Fus. Eng. Des., Vol. 75-79, p. 583 – 587, 2005.
[4] ITER Plant Description Document Chapter 2.4 "Divertor System", ref. G A0 FDR 1 01-07-13 R1.0, July 2001.
[5] ITER Design Description Document - Remote Handling Equipment WBS 23 - chapter 1, ref. N23 DDD 66 01-07-06 RO.2, july 2001.
[6] A. Fernandez-Fernandez, F. Berghmans, B. Brichard, P. Borgermans, A. Gusarov, M. Van Uffelen, P. Mégret, M. Decréton, M. Blondel, A. Delchambre, "Radiation-resistant WDM Optical Link for Thermonuclear Fusion Reactor Instrumentation", IEEE Trans. Nucl. Sci., Vol. 48, No. 5, pp. 1708-1712, 2001.
[7] M. Van Uffelen, A.Fernandez Fernandez, B. Brichard, F. Berghmans, M. Decréton, "Radiation tolerance qualification for maintenance tasks in the future fusion reactors: from fibre-optic components to robust data links", Fusion Engineering and Design, n°69, pp. 191-195, 2003.
[8] M. Van Uffelen, I. Genchev, F. Berghmans, "Wavelength dependence of the response of Si and InGaAs pin photodiodes under gamma radiation" (invited paper), Proceedings of the Conference on Photonics for Space Environments IX, SPIE Proceedings vol. 5554, pp. 132-143, 2004.
[9] A. Fernandez Fernandez, H. Ooms, B. Brichard, M. Coeck, S. Coenen, F. Berghmans, "Test Facilities at SCK•CEN for Radiation Tolerance Assessment: from space applications to fusion environments", proceedings of the 'RADECS 2002 Workshop', pp. 200-204, 2002.
[10] http://www.sckcen.be/BR1/
[11] E.J. Friebele, K.J. Long, C.G. Askins, M.E. Gingerich, M.J. Marrone, D.L. Griscom, "Overview of radiation effects in fiber optics", SPIE Vol. 541, pp 70-88, 1985.
[12] H. Nishikawa, R. Nakamura, R. Tohmon, Y. Ohki, "Y. Sakurai, K. Nagasawa, Y. Hama, "Generation

mechanism of photoinduced paramagnetic centers from preexisting precursors in high-purity silicas", Phys. Rev. B, Vol. 41, N°11, pp 7828-7834, 1990.

[13] H. Hanafusa, Y. Hibino, F. Yamamoto, "Formation mechanism of drawing-induced defects in optical fibres", J. Non-Cryst. Solids, N°95&96, pp 655-662, 1987.

[14] M. Van Uffelen, Y. El Shazly, S. Kukureka, G. Kuyt, E. Regnier, P. Matthijsse, F. Berghmans, " Mechanical reliability studies of optical fibres under high-dose gamma radiation", Proceedings of SPIE "Photonics Europe 2006: Optoelectronics and Photonic Materials" conference, SPIE Vol. 6193, 2006.

[15] F. Berghmans, K. Embrechts, M. Van Uffelen, S. Coenen, M. Decréton and J. Van Gorp, "Design and Characterization of a Radiation Tolerant Optical Transmitter using Discrete COTS Bipolar Transistors and VCSELs", IEEE Trans. Nucl. Sci., Vol. 49, No. 3, pp. 1414-1420, 2002.

[16] M. Van Uffelen, A. Giraud, F. Berghmans, " High gamma dose assessment of a multimode analogue fibre optic transmitter", Proceedings of the RADECS 2004 Workshop, 2004.

[17] K. Gill, C. Azevedo, J. Batten, G. Cervelli, R. Grabit, F. Jensen, J. Troska, F. Vasey, "Ageing tests of Radiation Damaged Lasers and Photodiodes for the CMS Experiment at CERN", proceedings of the RADECS 1999 conference, pp. 429-435, 2000.

[18] H. Ohyama, K. Takakura, K. Hayama, S. Kuboyama, Y. Deguchi, S. Matsuda, E. Simoen, C. Claeys, "Damage coefficient in high-temperature particle- and γ-irradiated silicon p-i-n diodes", Appl. Phys. Lett, Vol. 82, N° 2, pp. 296-298, 2003.

[19] K. Gill, V. Arbet-Engels, J. Batten, G. Cervelli, R. Grabit, C. Mommaert, G. Stefanini, J. Troska, F. Vasey, "Radiation Damage Studies of Optoelectronic Components for the CMS Tracker Optical Links", proceedings of the RADECS 1997 conference, pp 405-412, 1998.

[20] F. Berghmans, M. Van Uffelen, M. Decréton, " High total dose gamma and neutron radiation tolerance of VCSEL assemblies", SPIE Vol. 4823, pp. 162-171, 2002.

[21] M. Van Uffelen, K. Embrechts, F. Berghmans, S. Coenen, M. Decréton, J. Van Gorp, "Development of a high total radiation dose resistant vertical-cavity surface-emitting laser driver with discrete COTS components", SPIE Vol. 4547, pp. 94-104, 2001.

[22] M. Van Uffelen, M. Ortsiefer, J. Mols, F. Berghmans, "Ionizing radiation effects on long-wavelength VCSELs up to MGy dose levels ", Proceedings of the RADECS 2006 workshop, to be published.

[23] A. Giraud, "Radiation tolerance assessment of standard electronic components for remote handling", TWR-TV4-RADTOL annual activity report from CEA, ref. ra_tw4-tvr-radtol-2004.

[24] P. Leroux, M. Van Uffelen, F. Berghmans, A. Giraud, "Design and Assessment of a High Gamma-Dose Tolerant VCSEL Driver with Discrete SiGe HBT's", IEEE Trans. Nucl. Sci., Vol. xx, No. x, pp. xxxx-xxxx, 2005.

[25] M. Van Uffelen, S. Geboers, P. Leroux, F. Berghmans, "SPICE modelling of a discrete COTS SiGe HBT up to MGy dose levels", IEEE Trans. Nucl. Sci., Vol. xx, No. x, pp. xxxx-xxxx, 2005.

[26] P. Leroux, M. Van Uffelen, F. Berghmans, E. Simoen, C. Claeys, "A Compact, Broad-range, Physical SPICE Model Extension for the γ-radiation Induced β-degradation in a Discrete SiGe HBT", Proceedings of the RADECS 2006 workshop (to be published).

[27] P. Leroux, S. Lens, M. Van Uffelen, W. De Cock, M. Steyaert, F. Berghmans, " Design and Assessment of a Circuit and Layout Level Radiation Hardened CMOS VCSEL Driver", Proceedings of the RADECS 2006 workshop (to be published).

[28] S. Put, E. Simoen, E. Augendre, C. Claeys, M. Van Uffelen P. Leroux, " Comparison of the radiation behavior of 65 nm Fully Depleted Silicon-On-Insulator MOSFETs employing different tensile-strain-inducing techniques", Proceedings of the RADECS 2006 workshop (to be published).